

Induction of tumoricidal function in CD4⁺ T cells is associated with concomitant memory and terminally differentiated phenotype

Daniel Hirschhorn-Cymerman,¹ Sadna Budhu,¹ Shigehisa Kitano,⁵ Cailian Liu,¹ Feng Zhao,¹ Hong Zhong,¹ Alexander M. Lesokhin,^{1,2} Francesca Avogadri-Connors,¹ Jianda Yuan,⁵ Yanyun Li,¹ Alan N. Houghton,^{1,2,3} Taha Merghoub,¹ and Jedd D. Wolchok^{1,2,4,5}

¹Swim Across America Laboratory, Immunology Program, Sloan-Kettering Institute for Cancer Research, New York, NY 10065

²Weill Cornell Medical College and ³Graduate School of Medical Sciences of Cornell University, New York, NY 10065

⁴Ludwig Institute for Cancer Research, New York Branch, New York, NY 10065

⁵Ludwig Center for Cancer Immunotherapy at Memorial Sloan-Kettering Cancer Center, New York, NY 10065

Harnessing the adaptive immune response to treat malignancy is now a clinical reality. Several strategies are used to treat melanoma; however, very few result in a complete response. CD4⁺ T cells are important and potent mediators of anti-tumor immunity and adoptive transfer of specific CD4⁺ T cells can promote tumor regression in mice and patients. OX40, a costimulatory molecule expressed primarily on activated CD4⁺ T cells, promotes and enhances anti-tumor immunity with limited success on large tumors in mice. We show that OX40 engagement, in the context of chemotherapy-induced lymphopenia, induces a novel CD4⁺ T cell population characterized by the expression of the master regulator eomesodermin that leads to both terminal differentiation and central memory phenotype, with concomitant secretion of Th1 and Th2 cytokines. This subpopulation of CD4⁺ T cells eradicates very advanced melanomas in mice, and an analogous population of human tumor-specific CD4⁺ T cells can kill melanoma in an in vitro system. The potency of the therapy extends to support a bystander killing effect of antigen loss variants. Our results show that these uniquely programmed effector CD4⁺ T cells have a distinctive phenotype with increased tumoricidal capability and support the use of immune modulation in reprogramming the phenotype of CD4⁺ T cells.

CORRESPONDENCE

Jedd D. Wolchok:
wolchokj@mskcc.org

Abbreviations used: CTX, cyclophosphamide; Eomes, eomesodermin; GrzB, granzyme B; TDLN, tumor-draining LN; ViD, viability dye.

Current advances in T cell biology have challenged the notion that differentiated CD4⁺ T cells are irreversibly hardwired to a particular lineage as defined by the expression of specific transcription factors and cytokines. It is now clear that cellular microenvironments can phenotypically and functionally redirect a T cell population to different lineages (O'Shea and Paul, 2010). For example, recent evidence demonstrated that Foxp3⁺ regulatory T (T reg) cells and Th17 cells are interconvertible (Zhou et al., 2009). Even the more canonical Th1 and Th2 lineages can display unstable phenotypes (Hegazy et al., 2010). Furthermore, contrary to their traditionally defined roles, helper subsets have been shown to attain direct cytolytic properties

(Brown, 2010). An important consequence of the inherent plasticity of CD4⁺ T cells is that it can be exploited to elicit more potent immunotherapeutic effects such as in the context of adoptive T cell transfer to treat malignancies.

An important challenge in mobilizing an anti-tumor immune response is that the precursor frequency of T cells recognizing tumor antigens is very low (Moon et al., 2007; Rizzuto et al., 2009). Therefore, supplementing the host with tumor-specific T cells represents a logical approach (Grupp and June, 2011). Although extensive focus has been devoted to the study of CD8⁺ T cells in adoptive transfer protocols

T. Merghoub and J.D. Wolchok contributed equally to this paper.

© 2012 Hirschhorn-Cymerman et al. This article is distributed under the terms of an Attribution-Noncommercial-Share Alike-No Mirror Sites license for the first six months after the publication date (see <http://www.rupress.org/terms>). After six months it is available under a Creative Commons License (Attribution-Noncommercial-Share Alike 3.0 Unported license, as described at <http://creativecommons.org/licenses/by-nc-sa/3.0/>).

(Dudley et al., 2008; Rosenberg et al., 2008), CD4⁺ T cells have several potential advantages. CD4⁺ T cells can help orchestrate a global anti-tumor immune response by mobilizing numerous components of the immune system (Hunder et al., 2008; Muranski and Restifo, 2009). Furthermore, CD4⁺ T cells can acquire direct cytolytic activity under certain conditions, such as lymphopenia (Quezada et al., 2010; Xie et al., 2010).

It is well established that lymphopenia can enhance the potency of adoptive T cell therapies (Wrzesinski and Restifo, 2005). Cytotoxic agents, such as cyclophosphamide (CTX), induce lymphopenia and provide multiple immunomodulatory effects beneficial for adoptive T cell transfer (North, 1982; Bracci et al., 2007). CTX can remove suppressive cell populations (Awwad and North, 1988), sensitize tumor cells for immune destruction (van der Most et al., 2009), release tumor antigens and TLR agonists (Nowak et al., 2003; Apetoh et al., 2007), and promote homeostatic proliferation of transferred cells (Brode and Cooke, 2008).

Recent advances in immunotherapy have shown that checkpoint blockade with CTLA-4 and PD-1 blocking antibodies have resulted in significant clinical benefit in a variety of different malignancies (Brahmer et al., 2010; Wolchok et al., 2010). CTLA-4 blockade with ipilimumab produces an overall survival benefit in patients with metastatic melanoma, yet only 20–30% of patients seem to be sensitive to this intervention (Hodi et al., 2010; Robert et al., 2011). These recent advances in immune modulation, particularly checkpoint blockade with monoclonal antibodies, advocate for the incorporation of novel strategies that target T cell costimulation.

OX40 is a costimulatory molecule belonging to the TNFR family expressed primarily on activated effector T (T_{eff}) cells and naive T reg cells (Croft, 2010). Ligation of OX40, primarily on CD4⁺ T cells, activates NF- κ B and up-regulates antiapoptotic molecules from the Bcl-2 family, leading to T cell expansion, memory, activation, and cytokine secretion (Gramaglia et al., 2000; Rogers et al., 2001; Redmond et al., 2009). Furthermore, OX40 engagement on CD4⁺ Foxp3⁺ T reg cells leads to expansion, deactivation, or cell death depending on the local milieu (Colombo and Piconese, 2007; Vu et al., 2007; Hirschhorn-Cymerman et al., 2009; Ruby et al., 2009). Given that OX40 engagement can potentially stimulate T cells and potentially inhibit/eliminate T reg cells, OX40 agonists have been investigated in multiple preclinical tumor models (Weinberg et al., 2000; Piconese et al., 2008; Houot and Levy, 2009) and an anti-human OX40 monoclonal antibody is currently being evaluated in clinical trials (Clinical trial registration numbers NCT01303705 and NCT01416844; Weinberg et al., 2011). Despite this potential, targeting OX40 alone or in combination with other approaches has only shown effectiveness in preclinical models with low tumor burden.

We hypothesized that programming tumor-specific CD4⁺ T cells with an agonist OX40 antibody in the context of chemotherapy-induced lymphopenia would effectively treat more advanced tumors. Here, we show that OX40 engagement

in combination with CTX can promote transferred CD4⁺ T cells to durably regress very large tumors containing antigen loss variants. Closer examination revealed that OX40 ligation promoted the generation of highly cytolytic CD4⁺ T cells with a unique phenotype characterized by expression of markers of both terminal differentiation and memory, capable of secreting both Th1 and Th2 cytokines. In sum, the linear impact of this work extends from demonstration of the potency of optimally activated CD4⁺ T cells to the description of the phenotype of this novel population of effector cells.

RESULTS

CTX and OX86 synergize with anti-tumor CD4⁺ T cells to eradicate large established tumors

Previously, we showed that CTX in combination with OX40 engagement synergizes to regress established tumors (~0.2–0.4 cm in diameter; Hirschhorn-Cymerman et al., 2009). Given that OX40 preferentially provides costimulation to CD4⁺ T cells and CTX promotes lymphopenia, we hypothesized that the addition of tumor-specific CD4⁺ T cells would induce regression of more advanced tumors. To this end, mice bearing 3-wk-old B16 tumors (1.0–1.5 cm in diameter) were injected with CTX. The next day, purified CD4⁺ T cells from Trp1 transgenic mice (thereafter, Trp1 cells; Muranski et al., 2008) were transferred along with the anti-OX40 agonist antibody OX86 or IgG as a control. We found that all mice treated with the triple combination therapy (CTX + OX86 + Trp1 cells) durably eradicated tumors 3 wk after treatment (Fig. 1 A). Mice that received Trp1 cells, CTX, and IgG showed only temporary tumor regression. Mice treated with CTX and OX86 without Trp1 cells showed activity only in the subset of mice bearing small tumors. Mice that received CTX with IgG did not show any regression. The efficacy of the therapy was largely dependent on the number of Trp1 cells infused (unpublished data). Moreover, the triple combination therapy was effective in eliminating 3-wk-old JBRH melanoma and radically decreasing the tumor burden of TG3 and Grm1 spontaneous melanoma (unpublished data).

To further assess the potential clinical relevance of OX40 engagement in adoptive transfer protocols, we investigated whether other forms of immune modulation could enhance the anti-tumor potential of Trp1 cells. For that, we compared OX86 with anti-CTLA-4 (9D9), GITR (DTA-1), CD40 (FGK45), and PD-L1 (10F9G2). Although anti-CTLA-4 and anti-CD40 provided higher anti-tumor activity than controls, use of OX86 yielded significantly higher efficacy by regressing tumors in all recipients. Overall, these results show that adoptive transfer of anti-tumor CD4⁺ T cells synergizes with CTX and OX40 engagement to provide lasting anti-tumor immunity (Fig. 1 B).

Most adoptive transfer studies have focused on CD8⁺ T cells (Overwijk et al., 2003; June, 2007; Stromnes et al., 2010). For this reason, we compared the anti-tumor activity of CD8⁺ and CD4⁺ T cells in combination with CTX and OX86. Groups of mice bearing 3-wk-old tumors were pretreated with CTX and received equivalent numbers of Trp1 cells or

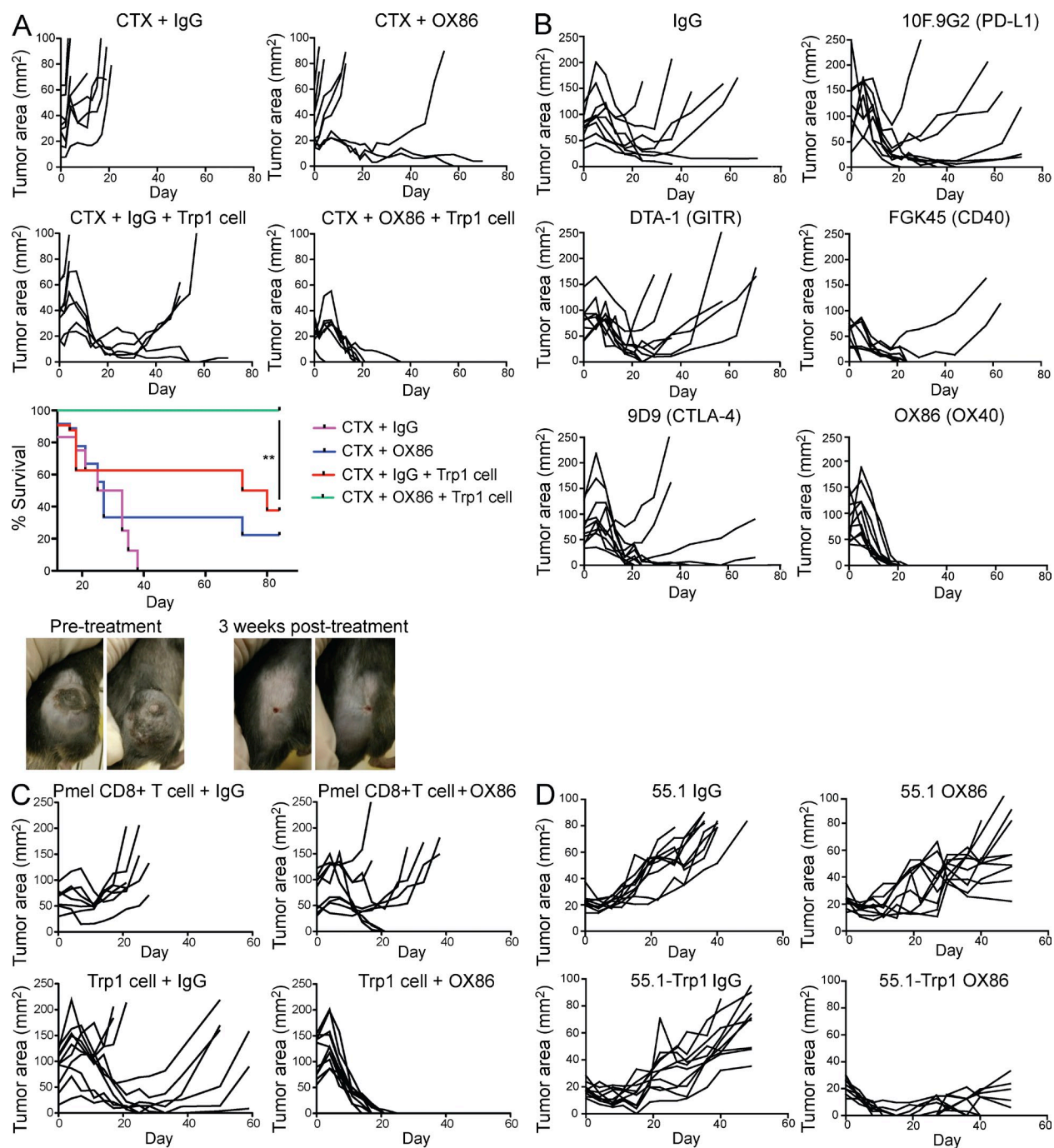


Figure 1. CTX and OX86 synergize with Trp1 CD4 T cells to eradicate large established tumors. (A) C57BL/6 mice (6–10/group) were inoculated intradermally in the flank with B16 cells. After 3 wk, mice were injected with CTX. The next day, mice were injected with OX86 (or IgG as control) with or without Trp1 cells as indicated. Tumors were measured periodically. Top: graphs represent tumor area of individual mice over time for each treatment. Middle: Kaplan-Meier overall survival curves. Bottom: representative photographs of mice treated with the triple combination therapy at day 0 or 21 after treatment. (B) C57BL/6 mice (7–11/group) inoculated intradermally in the flank with B16 cells. After 3 wk, mice were injected with CTX. The next day, Trp1 cells were transferred to all mice and groups were injected with 1 dose of agonist Abs (OX40, GITR, or CD40) or three doses of antagonist Abs (CTLA-4 or PD-L1) given 3 d apart. Tumor size was measured periodically. Graphs represent tumor area of individual mice over time for each treatment. (C) C57BL/6 mice (7–11/group) were inoculated intradermally in the flank with B16 cells. After 3 wk, mice were injected with CTX. The next day, Trp1 cells or Pmel-1 CD8⁺ T cells were injected and mice received OX86 (or IgG as control). Tumor size was measured periodically. Graphs represent tumor area of individual mice over time for each treatment. (D) C57BL/6 mice (10/group) were inoculated intradermally in the flank with Hep-55.1C or Hep-55.1C-Trp1 cells. On day 10, mice were injected with CTX. On day 11, mice received Trp1 cells and OX86 or IgG. Plots represent tumor area over time for each individual mouse. **, $P < 0.005$. All experiments were repeated at least twice with similar results.

CD8⁺ T cells from a TCR transgenic mouse specific for the melanoma antigen gp100 (Pmel-1 cells) followed by OX86 or rat IgG (Overwijk et al., 2003). Although OX86 improved the anti-tumor efficacy of Pmel-1 CD8⁺ T cells after CTX administration, the combination with Trp1 cells showed much higher anti-tumor activity (Fig. 1 C).

Given the potency of the combination therapy, we asked whether antigen expression in tumor cells is necessary because Trp1 cells can be activated by Trp1 protein expressed in melanocytes. We applied the combination therapy to cohorts of mice bearing established tumors from a hepatoma cell line expressing Trp1 (Hep55.1C-Trp1) or the parental cell line (Hep55.1C). Fig. 1 D shows that the combination therapy was only effective in mice bearing Hep55.1C-Trp1, confirming that antigen expression by the tumor is necessary for tumor elimination.

Combination therapy increases Trp1 T eff/T reg cell ratio by expanding T eff and reducing T reg cells via activation-induced cell death

Tumors may also evade immune elimination by recruiting and expanding CD4⁺ Foxp3⁺ T reg cells (Curiel, 2007). Strategies that eliminate T reg cells and, at the same time, increase T eff cells are therefore highly desirable as they improve the T eff/T reg cell ratio. Because a significant fraction of the transferred Trp1-specific transgenic cells express Foxp3 (Xie et al., 2010), we measured how CTX and OX86 therapy affects the Trp1 T eff/T reg cell ratio. Tumor-bearing mice were treated with CTX or PBS and, the next day, Trp1 cells were injected along with OX86 or IgG. On day 14 after treatment (when tumors show signs of regression), we found elevated T eff/T reg cell ratios that were several hundred-fold higher in both the tumor-draining LNs (TDLNs) and tumors in mice treated with CTX and OX86 compared with individual components of the combination therapy or control (Fig. 2 A). This dramatic increase in T eff/T reg cell ratio was caused by both profoundly decreasing the number of Trp1 Foxp3⁺ T reg cells (Fig. 2 D) and increasing Trp1 Foxp3⁻ T eff cells (Fig. 2 B).

Given our prior observation that the combination of CTX and OX86 promotes T reg cell-specific activation-induced cell death (Hirschhorn-Cymerman et al., 2009), we explored whether this mechanism is responsible for the decrease of Trp1 Foxp3⁺ T reg cells. Fig. 2 E shows that a larger percentage of Trp1-derived T reg cells stained positive for a viability dye (ViD) in both the tumors and TDLNs from mice treated with the CTX and OX86 compared with control. A majority of ViD⁺ Trp1 T reg cells costained with the proliferation marker Ki67 (Fig. 2 F), indicating that Trp1 T reg cells underwent activation-induced cell death. Although levels of Ki67 were high in Trp1 T eff cells treated with the combination therapy (Fig. 2 C), we did not detect higher apoptosis levels (not depicted), implying that activation-induced cell death was relatively specific for the T reg cell subpopulation. Furthermore, we found that elimination of

Trp1 T reg cells is partially FcR γ dependent. Levels of Trp1 T reg cells are significantly higher in tumors and TDLNs of FcR γ -deficient hosts (unpublished data).

OX40 engagement promotes enhanced Trp1 cell lytic function by up-regulation of eomesodermin (Eomes)

Several studies have shown that tumor-specific CD4⁺ T cells can acquire cytotoxic properties (Quezada et al., 2010; Xie et al., 2010). To assess if CTX and OX86 promote direct lytic potential of Trp1 cells, we applied the combination therapy to mice lacking mature T and B cells (Rag1^{-/-}) bearing B16 tumors. As shown in Fig. 3 A, the triple combination shows comparable efficacy in Rag1^{-/-} and wild-type hosts, suggesting that the transferred Trp1 cells directly kill B16 without the need for induction of an additional adaptive immune response. In addition, purified Trp1 cells from tumors, TDLNs, and spleens of mice treated with the combination therapy showed high ex vivo B16 cytotoxicity (Fig. 3 B and not depicted). These results indicate that the combination of CTX and OX86 enables Trp1 cells with direct tumoricidal activity.

Cytotoxic effector cells typically kill through FAS, TRAIL, or granzyme-perforin-dependent mechanisms (Trapani and Smyth, 2002). We sought to elucidate the primary mechanism responsible for the lytic activity of the Trp1 cells after CTX and OX86 combination therapy. For this, we measured surface expression of FAS and TRAIL on Trp1 cells ex vivo and did not find differences between OX86 treatment and control (unpublished data). However, Trp1 cells showed higher levels of CD107a and granzyme B (GrzB) in TDLNs, spleens, and tumors when exposed to CTX and OX86 (Fig. 3, C and D; and not depicted). Of interest, the endogenous CD4⁺ T cell population (CD45.1⁻) showed elevated levels of GrzB expression as well (Fig. 3 D). These results suggest that OX86 and CTX promote the cytotoxic potential of not only adoptively transferred CD4⁺ T cells but also endogenous CD4⁺ T cells.

The expression of GrzB and other lytic granules is under the control of the effector master regulator Eomes (Pearce et al., 2003). Recently, it has been reported that OX40 and 4-1BB engagement can induce the expression of Eomes on CD4⁺ T cells as well as differentiation to a Th1 phenotype (Qui et al., 2011). We therefore analyzed Eomes expression in CD4⁺ T eff cells after OX86 and CTX treatment. As shown in Fig. 3 E, a larger proportion of the Trp1 cells exposed to CTX and OX86 expressed both GrzB and Eomes compared with control. Interestingly, most GrzB⁺ cells were also Eomes⁺ suggesting that OX40-mediated GrzB expression is under the control of Eomes.

We then tested if similar induction of Eomes⁺ Trp1 cells results from treatment with other clinically relevant immune modulating antibodies. We treated mice with anti-CTLA-4 (9D9), anti-GITR (DTA-1), anti-CD40 (FGK45), and anti-PD-L1 (10F9G2) in addition to OX86 or control IgG after Trp1 cell transfer in tumor-bearing hosts pretreated with CTX. As shown in Fig. 3 F, only OX86 showed a substantial increase of Eomes⁺ Trp1 cells.

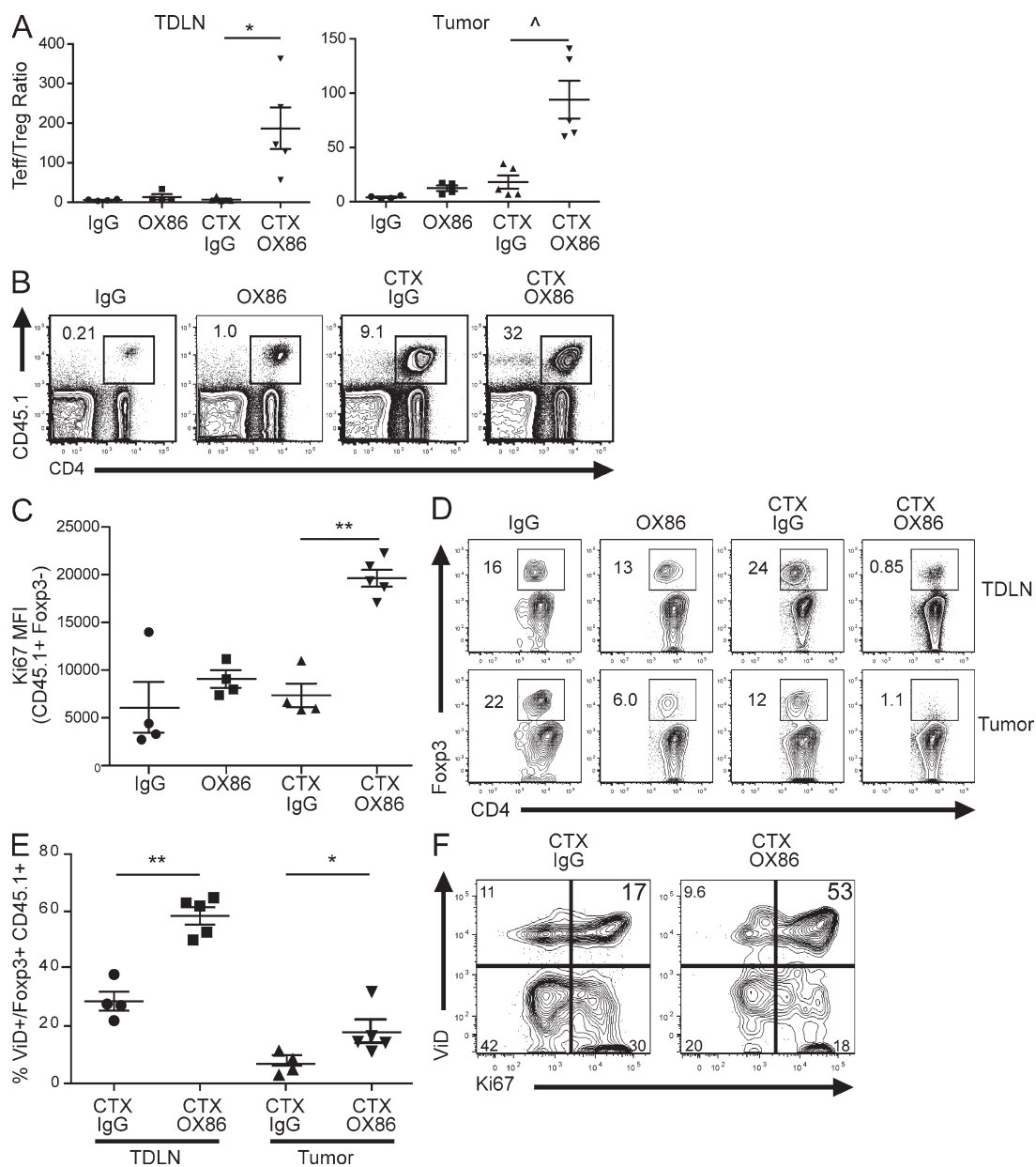


Figure 2. Combination therapy increases Trp1 T eff to T reg cell ratio by expanding T eff cells and reducing T reg cells via activation-induced cell death. C57BL/6 mice (4–5/group) were injected subcutaneously in the flank with B16 cells in Matrigel. 3 wk after tumor challenge, CTX or PBS was injected. The next day, Trp1 cells were transferred followed by injection of OX86 (or IgG as control). On day 14 after treatment, single cell suspensions were prepared from TDLNs and tumors. Cells were stained and analyzed by flow cytometry. (A) Graph represents T eff/T reg cell ratio \pm SEM in tumors and TDLNs. *, $P < 0.05$, ^, $P = 0.0599$. (B) Representative plots showing CD45.1 (Trp-1 cells) versus CD4 for each group pregated on ViD⁻ Fopx3⁻. ViD is a viability dye (ViD⁻: live cells). (C) Graph represents Ki67 MFIs \pm SEM of CD45.1⁺ CD4⁺ population in TDLNs. **, $P < 0.01$. (D) Representative plots of Fopx3 versus CD4 depicting the percentage of Trp1⁺ Fopx3⁺ in tumors and TDLNs. Events were pregated on ViD⁻ CD45.1⁺. (E) The graph represents the percentage of dead Trp1 T reg cells (ViD⁺ in the Fopx3⁺ CD45.1⁺ gate) in tumors and TDLNs. *, $P < 0.05$; **, $P < 0.01$. Error bars represent SEM. (F) Representative plots of activated dead Trp1 T reg cells ViD⁺ versus Ki67. Events were pregated on CD45.1⁺ Fopx3⁺. The experiments were repeated at least five times with equivalent results.

To test if Eomes up-regulation in Trp1 cells is necessary for the anti-tumor efficacy of the combination therapy, we knocked down Eomes expression in Trp1 cells by delivery of an Eomes shRNA-GFP encoding retrovirus. After 5 d in culture, cells were FACS sorted for GFP^{high} expression and analyzed by

flow cytometry. We found a profound reduction of Eomes and GrzB, but not the related gene T-bet, in Eomes shRNA transduced cells compared with control retrovirus transduced cells (Fig. 3 G). Functionally, Eomes shRNA transduced cells show reduced B16 killing in an in vitro cytotoxicity assay (Fig. 3 H).

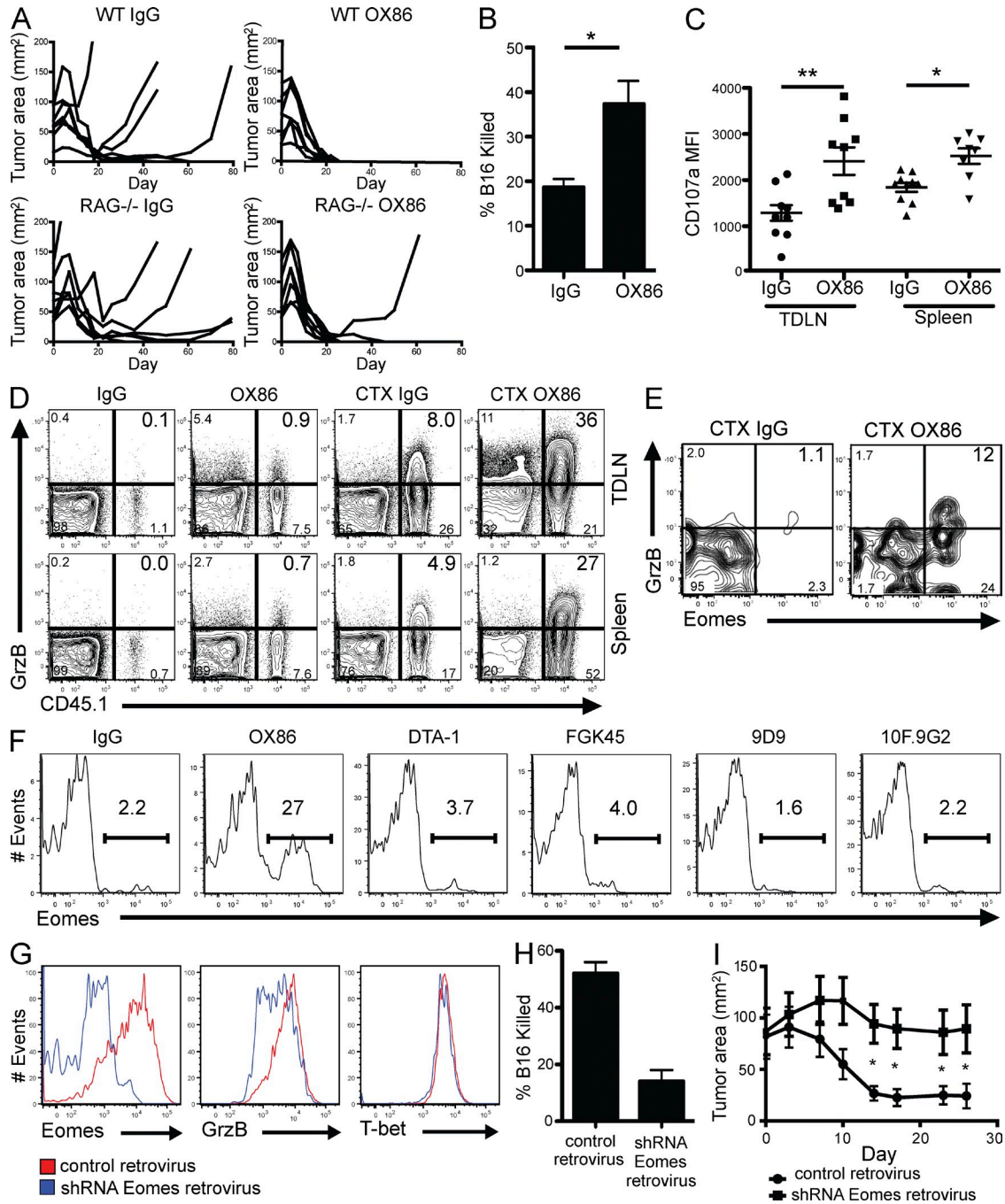


Figure 3. Direct cytotoxicity by Trp1 cells as a result of OX40 engagement during CTX-induced lymphopenia is Eomes dependent.

(A) C57BL/6 wild-type or Rag1^{-/-} mice (6–10/group) were inoculated intradermally in the flank with B16 cells. After 3 wk, mice were injected with CTX, followed the next day by OX86 (or IgG as control) and Trp1 cells. Tumors were measured periodically. Graphs represent tumor area of individual mice over time for each treatment. (B) C57BL/6 mice (10 mice/group) were injected subcutaneously with B16 in Matrigel. 3 wk after tumor challenge, CTX was injected. The next day, mice were injected with Trp1 cells and OX86 (or IgG). On day 14 after treatment, Trp1 cells were purified by FACS from splenocytes and were used for in vitro killing assays using B16 cells as targets at a 10:1 effector to target ratio. Means of three individual wells and SEM are shown. *, P < 0.05. (C) Single cell suspensions of TDLNs and spleens from mice that were treated, as in B (8 mice/group), were stimulated overnight with Trp1 peptide in the presence of monensin and anti-CD107a-FITC. The next day, the samples were stained for CD45.1 (Trp1 cells) and other phenotypic markers and analyzed by flow cytometry. Plots show CD107a MFIs of individual mice gated on ViD⁻ CD45.1⁺ CD4⁺ Foxp3⁻. *, P < 0.005; **, P < 0.05. Error bars represent SEM. (D) Single cell suspensions of TDLNs and spleens from mice that were treated as in B (4–5 mice/group) were stained and analyzed by flow cytometry for GrzB and other phenotypic markers on day 14 after treatment. Representative plots are shown for GrzB versus CD45.1. Events were pregated on ViD⁻, CD4⁺, and Foxp3⁻. (E) C57BL/6 mice (7–10/group) were treated as in B and bled on day 14 after treatment. PBMCs were stained for GrzB and Eomes and analyzed by flow cytometry. Events were pregated on ViD⁻, CD45.1⁺, CD4⁺, and Foxp3⁻.

To establish if Eomes is necessary for the potency of the combination therapy, we injected OX86 and transferred Trp1 cells transduced with Eomes shRNA or empty virus into Rag1^{-/-} mice bearing large established B16 tumors pretreated with CTX. As shown in Fig. 3 I, mice treated with Trp1 cells transduced with empty retrovirus showed significant tumor regression, whereas mice treated with Eomes shRNA transduced Trp1 cells exhibited lower anti-tumor activity. Overall, these results show that the combination of CTX and OX86 enable CD4⁺ T eff cells to acquire a cytotoxic phenotype, at least in part, via Eomes.

CTX and OX86 promote the expression of terminal differentiation and memory markers and the secretion of both Th1 and Th2 cytokines in Trp1 cells

Cytotoxic CD4⁺ T cells are typically associated with markers of terminally differentiated short-lived effectors (Brown, 2010). However, Eomes expression has recently been linked to the formation of memory in CD8⁺ T cells (Banerjee et al., 2010; Zhou et al., 2010). Moreover OX40 engagement on CD4⁺ T cells can promote clonal expansion and memory (Croft, 2010). To reconcile these potential disparities, we phenotyped single cell suspensions from TDLNs of treated mice by staining for markers associated with terminal differentiation and memory. As shown in Fig. 4 A, Trp1 Foxp3⁻ T eff cell exposed to the combination therapy expressed higher levels of Eomes (as expected) but also higher levels of Klrp1 and lower levels of Bcl-6, markers typically associated with cytolytic potential/terminal differentiation (Belz and Kallies, 2010; Crotty et al., 2010; Fig. 4 A). Interestingly, the combination therapy also modulated the expression of markers consistent with increased memory and less exhausted phenotypes on Trp1 CD4⁺ Foxp3⁻ T eff cell: CD127^{high}, T-bet^{low}, CD62L^{high}, and PD-1^{low} (Belz and Kallies, 2010; Wherry, 2011; Fig. 4 A). A similar expression pattern was observed in the endogenous CD4⁺ Foxp3⁻ T eff cell population (unpublished data). These results indicate that OX86 engagement can induce a unique CD4⁺ T cell population to concomitantly acquire both cytolytic effector and memory phenotypes.

Because CD4⁺ T eff cells differentiate into distinct lineages with unique cytokine profiles, we examined how CTX and OX86 influenced Trp1 T eff cytokine expression within

the tumor microenvironment. To this end, we incubated purified Trp1 cells from tumors and TDLNs of treated mice in the presence of APCs and Trp1 peptide. After 4 d in culture, the supernatants were tested for the secretion of Th1, Th2, and Th17 cytokines. Surprisingly, we found that Trp1 cells exposed to OX86 secreted higher levels of both Th1 (IL-2, IFN- γ , and TNF) and Th2 (IL-4, IL-5, and IL-13) cytokines but produced insignificant levels IL-17 (Fig. 4 B). A possible explanation is that purified Trp1 cells could include separate populations of Th1 and Th2 cells. We therefore tested if Trp1 cells can concomitantly secrete both sets of cytokines by intracellular cytokine staining. We found that a large proportion of Trp1 T eff cells secreted IFN- γ and TNF (Fig. 4 C–E) and the majority of cells secrete both cytokines simultaneously, consistent with a polyfunctional Th1 phenotype. Moreover, Trp1 T eff cells exposed to the combination therapy also secreted IL-4 (Fig. 4 F), with the majority of cells secreting IL-4 also secreting IFN- γ (Fig. 4 G). Furthermore, OX86 treatment reduced the levels of IL-17-secreting Trp1 T eff cells (Fig. 4 H). Overall, these results suggest that CTX and OX86 promote Trp1 CD4⁺ T eff cells to secrete both Th1 and Th2 cytokines while modestly inhibiting a Th17 lineage.

Triple combination therapy promotes bystander killing of antigen loss variants

Tumors may be populated by cells that lose expression of antigenic proteins (Dunn et al., 2002; Spiotto et al., 2004). This heterogeneity not only is a predominant mechanism to avoid immune destruction but also renders immunotherapies that target a single antigen eventually ineffective. For this reason, we tested whether the combination of CTX and OX86 induces Trp1 cells to eliminate tumors containing cells which do not consistently express the cognate antigen (Trp1). We injected groups of mice with a mixture of B16 melanoma cells and B78H1, a B16 clone which does not express the Trp1 protein (Graf et al., 1984). As controls, we injected mice with B16 or B78H1 alone or both cell lines in different flanks, and the triple combination therapy was applied (Fig. 5, scheme). We found that the triple combination therapy eradicated pure B16 tumors, as expected, but was ineffective in treating B78H1 tumors (Fig. 5). Moreover, when B16 and B78H1 were injected in different flanks on the same mouse, only B16 regressed

Representative plots are shown of GrzB versus Eomes. (F) C57BL/6 mice (4–5/group) were injected subcutaneously with B16 in Matrigel. 3 wk after tumor challenge, CTX was injected. The next day, mice were injected with Trp1 cells and OX86, DTA-1, FGK45, 9D9, 10F.9G2, or IgG. Two additional doses of 9D9 and 10F.9G2 were given every 3 d. On day 14 after treatment, single cell suspensions were stained for Eomes and other phenotypic markers and analyzed by flow cytometry. Events were gated on ViD⁻, CD45.1⁺, CD4⁺, and Foxp3⁻. Representative plots are shown of GrzB versus Eomes. (G) In vitro activated Trp1 cells were transduced with Eomes shRNA-GFP retrovirus or GFP retrovirus as control. Transduced cells were FACS sorted on GFP^{high} gate 5 d later. Cells were stained intracellularly for Eomes, GrzB, and T-bet and analyzed by flow cytometry. Representative histograms are shown. (H) In vitro cytotoxicity assay with transduced Trp1 cells sorted on GFP^{high} gate. B16 cells were used as targets at a 10:1 effector to target ratio. Bars represent the means of duplicate wells and the SEM is shown. (I) C57BL/6 Rag1^{-/-} mice (6/group) were inoculated intradermally in the flank with B16 cells. 3 wk later, CTX was injected followed the next day by the transfer of 70,000 transduced Trp1 cells (sorted on GFP^{high}) and injection of OX86. Tumor area was periodically monitored. Each point represents the mean tumor area and error bars are SEM. *, P < 0.05. All experiments were repeated at least twice with similar results.

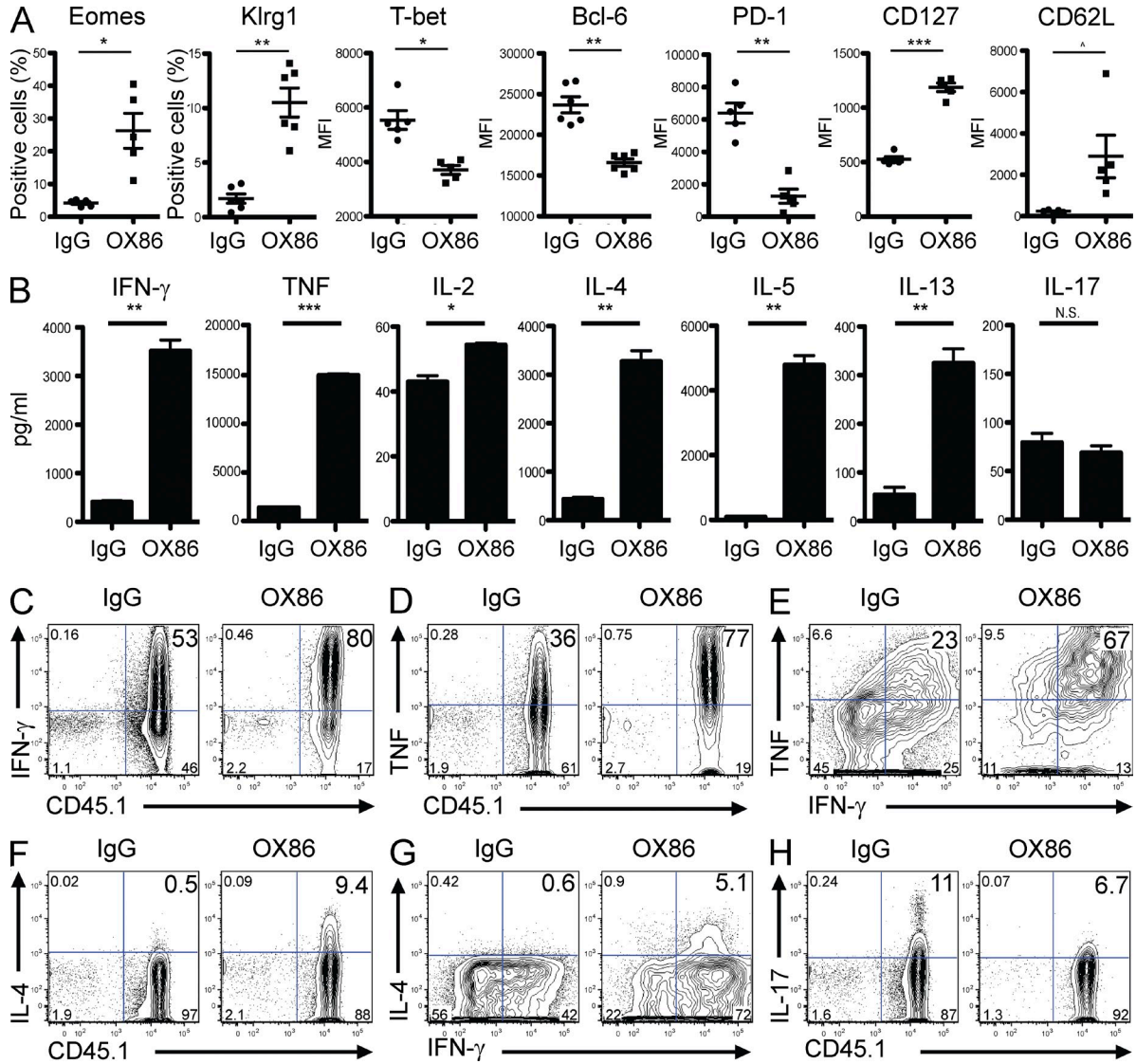


Figure 4. CTX and OX86 promotes Trp1 cells to acquire terminal differentiation and memory phenotype with mixed Th1/Th2 cytokine secretion. (A) C57BL/6 mice (4–5 mice/group) were injected subcutaneously in the flank with B16 in Matrigel. 3 wk after tumor challenge, CTX was injected. The next day, Trp1 cells were transferred followed by injection of OX86 or IgG. On day 14 after treatments, single cell suspensions from TDLNs were stained and analyzed by flow cytometry for Eomes, Klrp1, Bcl-6, T-bet, PD-1, CD127, and CD62L. Events were pregated on ViD⁻ CD4⁺ CD45.1⁺ Foxp3⁻. *, P < 0.05; **, P < 0.005; ***, P < 0.0005; ^, P = 0.0632. Experiment was repeated at least three times with similar results. Error bars represent SEM. (B) C57BL/6 mice (10 mice/group) were injected subcutaneously in the flank with B16 in Matrigel. 3 wk after tumor challenge, CTX was injected. The next day, Trp1 cells were transferred followed by injection of OX86 or IgG. On day 14 after treatments, tumors from each group were pooled and single cell suspensions were prepared. Trp1 cells were purified by MACS and co-cultured with irradiated APCs (pulsed with Trp1 peptide). After 4 d, cytokine levels were measured in supernatants by cytokine bead arrays. Graphs show the means \pm SEM of three individual wells per condition. *, P < 0.05; **, P < 0.01; ***, P < 0.001. (C–H) C57BL/6 mice (4–5 mice/group) were injected subcutaneously in the flank with B16 in Matrigel. 3 wk after tumor challenge, CTX was injected. The next day, Trp1 cells were transferred and injected with OX86 (or IgG). On day 14 after treatment, single cell suspensions were prepared from tumors and incubated for 8 h in the presence of APCs pulsed with Trp1 peptide. The cells were stained and analyzed by intracellular flow cytometric analysis. (C) Representative plot of IFN- γ versus CD45.1. Events were pregated on ViD⁻ CD4⁺ Foxp3⁻. (D) Representative plot of TNF versus CD45.1. Events were pregated on ViD⁻ CD4⁺ Foxp3⁻. (E) Representative plot of TNF versus IFN- γ . Events were pregated on ViD⁻ CD4⁺ Foxp3⁻ CD45.1⁺. (F) Representative plot of IL-4 versus CD45.1. Events were pregated on ViD⁻ CD4⁺ Foxp3⁻. (G) Representative plot of IL-4 versus IFN- γ pregated on ViD⁻ CD4⁺ Foxp3⁻ CD45.1⁺. (H) Representative plot of IL-17 versus CD45.1 pregated on ViD⁻ CD4⁺ Foxp3⁻. Experiments were repeated at least three times with similar results.

whereas B78H1 was unaffected. Interestingly, the majority of B16:B78H1 chimeric tumors (7/8) regressed, indicating that the combination therapy can eliminate tumors by triggering a

local bystander killing effect on tumor cells not expressing cognate antigen. This observation is of potential clinical importance given tumor heterogeneity.

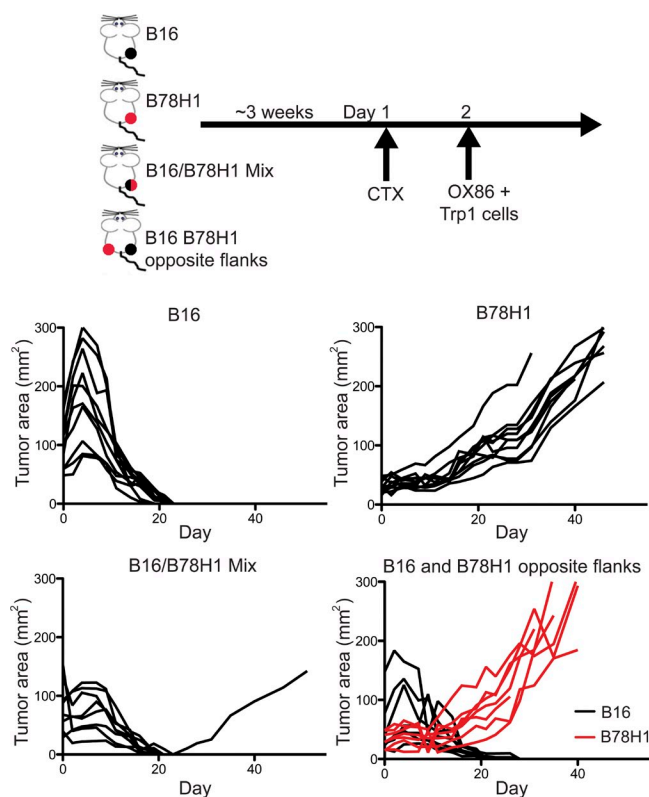


Figure 5. Triple combination therapy promotes bystander tumor killing of antigen loss variants. C57BL/6 mice (8/group) were inoculated intradermally in the flank with B16 cells, B78H1, B16, and B78H1 in opposite flanks, or a B16:B78H1 mixture. 3 wk later, CTX was injected followed the next day by treatment with Trp1 cells and OX86 as described in the top diagram. Graphs represent tumor area of individual mice over time for each treatment. Similar results were obtained in two individual experiments.

Human NY-ESO-1-specific CD4⁺ T cell lines exhibit enhanced killing of melanoma cell lines when exposed to OX40 agonist in vitro

We further asked if OX40 engagement could enhance the tumoricidal activity of human CD4⁺ T cells. First, we set up in an in vitro system to assess whether OX40 ligation is sufficient to enhance direct tumor cell killing by Trp1 cells. Trp1 cells activated with peptide-pulsed APCs in the presence of OX86 were subjected to an in vitro cytotoxicity assay and the killing potential of cells treated with OX86 was increased threefold (Fig. 6 A). With this system in place, CD4⁺ T cell lines specific for NY-ESO-1 derived from three patients with advanced melanoma (unpublished data) were expanded with plate-bound anti-CD3 in the presence or absence of human agonist OX40L-Fc protein. After 10 or 14 d in culture, the CD4⁺ T cell lines were tested for cytotoxic potential using patient-matched melanoma cell lines as targets. As shown in Fig. 6 B, OX40 engagement significantly enhanced the cytotoxicity of all NY-ESO-1-specific CD4⁺ T cell lines to levels equivalent to the Trp1 cells. Moreover, RT-PCR analysis revealed a phenotype comparable to Trp1 cells, with the exception

of T-bet and PD-1 (Fig. 6 C). These discrepancies could be a result of differences in human OX40 signaling or in vitro culture conditions. Overall, these results highlight the translational potential of OX40 engagement in promoting and/or enhancing anti-tumor cytotoxic CD4⁺ T cells.

DISCUSSION

We have demonstrated that in vivo engagement of OX40 in the context of adoptive transfer of antigen-specific CD4⁺ T cells is a potent approach that can completely and durably regress advanced B16 melanoma tumors. Our results show that in this context, the OX40 agonist antibody provides superior anti-tumor efficacy compared with other immunomodulatory antibodies when combined with CTX and antigen-specific CD4⁺ T cells. Under the same conditions, antigen-specific CD4⁺ T cells achieve higher potency than antigen-specific CD8⁺ T cells. The efficacy of this therapy was accompanied by increasing Trp1 CD4⁺ T eff cells and reducing T reg cells, resulting in a favorable T eff/T reg cell ratio within the tumor microenvironment.

Several attempts have been made to engineer T cells from patients in vitro to increase tumoricidal activity. Our results imply that in vivo modulation with antibodies provides an alternative in reprogramming transferred cells to improve clinical outcomes. The availability of immunomodulatory antibodies enhances the feasibility of this approach.

To confirm the clinical applicability of our findings, we established an in vitro system in which the ability of OX40 engagement to increase the tumoricidal capability of human antigen-specific T cells was tested. NY-ESO-1-specific CD4⁺ T cell lines exposed to a human OX40 agonist increased their ability to lyse autologous melanoma cells, supporting the cytolytic phenotype observed in mouse models.

The selective pressure that the adaptive immune system exerts on tumors leads to antigen down-regulation (Dunn et al., 2002; Spiotto et al., 2004). This important escape mechanism poses a challenge when targeting a single antigen. We found, however, that local destruction of tumor cells lacking the target antigen (Trp1) is possible when potent immunotherapies mediate sufficient bystander killing. Although the precise mechanisms leading to the observed effect are currently elusive, it is unlikely that systemic epitope spreading is responsible for the regression of mixed B16:B78H1 tumors because B78H1 tumors were not eliminated when injected concomitantly with B16 at a distant site. We hypothesize that Trp1 cells exposed to OX86 and CTX infiltrate tumors, directly killing antigen-expressing cells and, at the same time, promote a favorable local inflammatory milieu that recruits innate cells eliminating antigen escape variants and/or stromal cells.

Our results indicate that, under CTX-induced lymphopenic conditions, OX40 engagement promotes Trp1 cells as well as endogenous CD4⁺ T cells to acquire a highly cytotoxic phenotype by inducing Eomes. However, the endogenous CD4⁺ T cell population is not necessary for eliminating tumors because regression could be recapitulated in mice

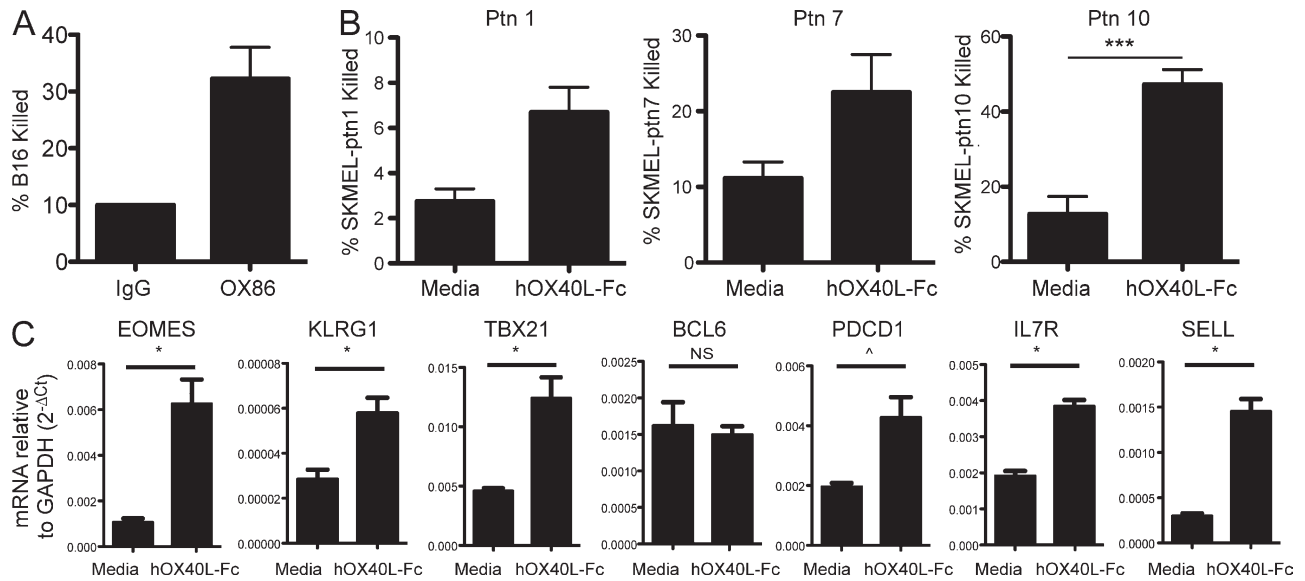


Figure 6. Human and mouse tumor-specific CD4⁺ T cells showed enhanced anti-tumor lytic activity with OX40 ligation in vitro. (A) Purified Trp1 cells were incubated with APCs and Trp1 peptide and, 48 h after incubation, 10 μg/ml OX86 (or IgG as control) was added to the cultures. After 5 d, the cells were subjected to in vitro cytotoxicity assay using B16 cells as targets at 10:1 effector to target ratio. Graphs show the mean percent killing of duplicate wells. Error bars represent SEM. (B) NY-ESO-1-specific CD4⁺ T cell lines from three different patients were expanded with plate-bound anti-CD3 and IL-2 in the presence or absence of 10 ng/ml of recombinant human OX40L-Fc. After 10 or 14 d in culture (ptn 1 or 7 and 10, respectively), the CD4⁺ T cell lines were subjected to an in vitro cytotoxicity assays using patient-matched melanoma cell lines (SKMEL-ptn 1, 7, and 10) pulsed with NY-ESO-1 peptide pools as targets. Bars depict the means of percentage of targets killed of duplicate or triplicate wells/treatment. Errors bars represent SEM. ***, P = 0.0004. Experiments were repeated at least three times with similar results. (C) NY-ESO-1-specific CD4⁺ T cell lines (patient 7) were expanded with plate-bound anti-CD3/CD28 and IL-2 in the presence or absence of 5 ng/ml of recombinant human OX40L-Fc. After 7 d, RNA was extracted and subjected to RT-PCR for *EOMES* (Eomes), *KLRG1* (KLRG1), *TBX21* (T-bet), *BCL6* (Bcl-6), *PDCD1* (PD-1), *IL7R* (CD127), and *SELL* (CD62L). Graphs represent means of triplicate wells/treatment. Error bars represent SEM. *, P < 0.05; ^, P = 0.056. Experiments were repeated at least twice with similar results in cell lines derived from two patients.

lacking the capacity to generate adaptive immunity (Rag1^{-/-}). Moreover, the observation that CD4⁺ T cells with the newly described phenotype have potent direct anti-tumor properties suggests that this approach could be a means to potentiate engineered T cells.

Given that Trp1 cells—in the context of OX40 engagement and lymphopenia—durably control advanced tumors, we further characterized and defined the phenotypic “fingerprint” of these uniquely potent cells. Cytotoxic CD4⁺ T cells can develop under conditions of chronic antigen exposure leading to a terminally differentiated phenotype (Brown, 2010). However, upon OX40 stimulation, Trp1 cells not only acquire a terminally differentiated phenotype (Klrg-1^{high} and Bcl-6^{low}) but also exhibit markers correlated with memory/low exhaustion (CD62L^{high}, T-bet^{low}, CD127^{high}, and PD-1^{low}; Belz and Kallies, 2010; Wherry, 2011). A recent study showed that Eomes expression enables CD8⁺ T cells to acquire both effector and memory/self-renewal functions (Banerjee et al., 2010). An intriguing hypothesis is that the inherent plasticity in both CD4⁺ and CD8⁺ T cells allows for the possibility of developing even more potent cells for clinical use when properly stimulated.

The cytokine profile of anti-tumor CD4⁺ T cells exposed to the combination therapy reveals both Th1 and Th2 cytokine secretion. As opposed to other studies (Qui et al., 2011)

where OX40 and 4-1BB engagement were shown to drive cytotoxic Th1 differentiation, here we show that secretion of both Th1 and Th2 cytokines is a hallmark of our newly described CD4⁺ T cell population. This difference in CD4⁺ T cell phenotype may explain the superior anti-tumor efficacy with the conditions described in our manuscript. Moreover, we found that OX86 diminished Th17 and TFh (T follicular helper) lineages, shown by lower levels of IL-17 and down-regulation of Bcl-6 (Johnston et al., 2009). Although Eomes can inhibit RoRγt, which could account for IL-17 down-regulation (Ichiyama et al., 2011), the observation that Trp1 cells secrete both Th1 and Th2 cytokines under these conditions is perplexing. Given that T-bet represses Th2 cytokines such as IL-4 to promote Th1 polarization (Zhu et al., 2010), it is feasible that T-bet down-regulation overcomes IL-4 suppression and high Eomes expression promotes IFN-γ secretion. Moreover, several experiments in viral models where CD4⁺ T cells were polarized into different helper lineages (Th0, Th1, Th2, and Th17) show that cells with the Th0 phenotype exhibit higher cytotoxic potential (Brown, 2010). We speculate that OX40 engagement drives Trp1 cells to acquire a highly cytotoxic Th0-like phenotype in vivo, characterized by Eomes expression. This suggests that OX40 engagement may induce a new effector Th lineage which warrants further characterization.

Overall, our observations highlight the clinical potential of OX40 engagement in promoting a cytotoxic CD4⁺ T cell population with unique phenotypic markers. As adoptive transfer of designer or engineered cells becomes more feasible, optimizing their anti-tumor potential is of clear importance. The ability to modulate cells with sufficient lineage plasticity in vivo with a single monoclonal antibody opens a new avenue and overcomes many of the challenges encountered by adoptive T cell therapy protocols.

MATERIALS AND METHODS

Mice and tumor cell lines. All mouse procedures were performed in accordance with institutional protocol guidelines at Memorial Sloan-Kettering Cancer Center (MSKCC) under an approved protocol. C57BL/6j or C57BL/6j Rag1^{-/-} (8–10-wk-old males) were obtained from The Jackson Laboratory. Pmel-1 TCR transgenic mice (Overwijk et al., 2003) and Trp1 CD4⁺ TCR transgenic mice (Muranski et al., 2008) were obtained from the N. Restifo laboratory (National Institutes of Health, Bethesda, MD). Trp1 CD4⁺ TCR transgenic were crossed to Rag1^{-/-} Trp1^{-/-} CD45.1 background. All mice were bred at MSKCC. The B16-F10 mouse melanoma line was originally obtained from I. Fidler (M.D. Anderson Cancer Center, Houston, TX). B78H1 was obtained from A. Albino (Sloan-Kettering Institute). Inoculation with 10⁵ B16-F10 or 10⁶ B78H1 cells was determined to be a lethal dose when injected intradermally in the flank (50 µl/injection). In experiments where B16-F10 and B78H1 were co-injected, the lethal dose for each tumor was mixed in the same volume. For experiments where isolation of tumor lymphocytes was performed, B16-Matrigel was subcutaneously injected (10⁵ B16-F10 cells in 0.2 ml of Matrigel Matrix Growth Factor Reduced; BD). Parental Hep 55.1C (Kress et al., 1992) was a gift from M. Schwarz (University of Tübingen, Tübingen, Germany). Hep 55.1C-Trp1 were prepared by transfection with pCRAN-mgp75 and stable Trp1-expressing clones were selected after treatment with 1 mg/ml G418 (Gibco). Trp1 expression was confirmed by Western blotting. 1 × 10⁵ cells were titrated to be a lethal dose.

Monoclonal antibodies, drug treatment, and adoptive transfer experiments. OX86 (anti-OX40; al-Shamkhani et al., 1996), FGK45 (anti-CD40; Rolink et al., 1996), and DTA-1 (anti-GITR; Ko et al., 2005) were produced and purified by the Monoclonal Antibody Core Facility at MSKCC. 9D9 (anti-CTLA-4; Quezada et al., 2006) and 10F9G2 (anti-PD-L1; Eppihimer et al., 2002) were purchased from BioXcell. Anti-rat IgG (Sigma-Aldrich) was reconstituted in sterile PBS before injection. For all treatments, a single dose of 0.5 mg OX86, 0.5 mg rat IgG, 0.25 mg FGK45, and 1 mg DTA-1 was injected. Three doses of 0.1 mg 9D9 and 0.2 mg 10F9G2 were administered every 3 d. CTX monohydrate (Sigma-Aldrich) mixed in sterile PBS was administered as a single dose at 250 mg/kg. Both agents were administered intraperitoneally. Trp1 CD4⁺ T cells (Trp1 cells) or Pmel-1 CD8⁺ T cells were purified from LN and spleen by positive selection magnetic cell sorting using CD4 beads (L3T4) or CD8 (Lyt2; Miltenyi Biotech) according to the manufacturer's instructions. Unless stated, 1 × 10⁵ purified Trp1 T cells or Pmel-1 CD8⁺ T cells were tail vein injected.

FACS analysis and cell sorting. The following antibodies were used for flow cytometry analysis: CD4 Pacific blue, Ki67 FITC, CD107a FITC, IL-17 PE, TNF APC, and PE-Texas red Streptavidin were obtained from BD. PD-1 Biotin, Eomes PE, T-bet PercpCy5.5, CD45.1 APC-eFluor 780, CD62L PerCP-Cy5.5, Foxp3 APC, Foxp3 FITC, Klrp1 PE-Cy7, CD127 PE-Cy7, Bcl-6 PE, IFN-γ PerCP-Cy5.5, and IL-4 PE-Cy7 were obtained from eBioscience. GrzB PE-TX and ViD (LIVE/DEAD Fixable Aqua Dead Cell Stain kit) were obtained from Invitrogen. All antibodies were used according to the manufacturer's instructions with the recommended buffers.

Lymphocytes from tumors were prepared by digestion in 1× Liberase/DNase (Roche) solution in plain RPMI 1640 for 30 min at 37°C. After passing the solution through a 40 µm filter, live lymphocytes were isolated using

Percoll (GE Healthcare) gradient centrifugation as described in Hirschhorn-Cymerman et al. (2009). Cells from TDLNs and tumors were prepared by mechanical dissociation in 40 µm filters and red blood cells were removed by incubation in ACK Lysing Buffer (Lonza). For CD107a mobilization assay, lymphocytes from TDLNs and spleens were incubated at 37°C with 2.5 µg/ml of Trp1 peptide in HTM medium (RPMI 1640 supplemented with 10% FCS, 1× nonessential amino acids, 1 mM sodium pyruvate, 2 mM L-glutamine, and 50 µM β-mercaptoethanol) overnight with 10 µg/ml of monensin (Sigma-Aldrich) and 1 µl of CD107a FITC. For intracellular cytokine staining, lymphocytes from tumors were incubated at 37°C with 2.5 µg/ml of Trp1 peptide in HTM medium for 8 h with 10 µg/ml monensin and 1X GolgiPlug (BD). Before staining, cells were treated with saturating anti-CD16/CD32 (BD) in staining buffer (2% bovine serum albumin and 2 mM EDTA in PBS) on ice for 15 min. Staining of surface antigens was performed in staining buffer on ice for 40 min. All intracellular staining was conducted using the Foxp3 fixation/permeabilization buffer (eBioscience) according to the manufacturer's instructions. Flow cytometry was performed on an LSR II (BD). FlowJo software (version 9.4.10; Tree Star) was used for all flow cytometry analysis. FACS sorting was conducted on a FACSAria II cell sorter (BD).

Peptides. Trp1 peptide (Muranski et al., 2008) was synthesized by Genemed Synthesis, Inc. Overlapping NY-ESO-1 peptides (20-mers overlapping by 10 peptides), were purchased from JPT Peptide Technologies.

Retrovirus construction and transduction. Four candidate Eomes shRNA sequences and control psHIVN-H1 lentivirus backbone were obtained from GeneCopoeia with the following specific sequence: Eomes1, 5'-ACAAAGCGTCCAAGAAGTT-3'; Eomes2, 5'-CAAAGCGGACAAT-AACATG-3'; Eomes3, 5'-GCACTCTCTGCACAAATAC-3'; Eomes4, 5'-CTGTGACCAACAAGCTAGA-3'; or scrambled shRNA. The psHIVN-H1 lentivirus plasmids were cotransfected with Fugene 6 (Roche) with full-length Eomes in MigR1 backbone (gift of S. Reiner, University of Pennsylvania, Philadelphia, PA) into HEK 293 cells in 6-well plates. After 48 h, the cells were fixed and permeabilized with Cytotfix/Cytoperm (BD), stained for Eomes, and analyzed by flow cytometry. shRNA Eomes4 sequence almost entirely inhibited Eomes expression and was further used for subsequent experiments. Because of our inability to effectively transduce activated CD4⁺ T cells with a lentivirus, the shRNA Eomes4 sequence was subcloned into MigR1 retrovirus backbone and was called Eomes shRNA-GFP thereafter. Transduction of Trp1 cells was performed as described by Lee et al. (2009). In brief, purified CD4⁺ T cells from TDLNs and spleens of Trp1 mice were activated with T cell-depleted, irradiated splenocytes (APCs) pulsed with 2.5 µg/ml of Trp1 peptide at 1:3 ratio in HTM media supplemented with 50 U/ml of recombinant human IL-2 (Roche). After 2 d in culture, the activated CD4⁺ T cells were inoculated with high titer virus solution of Eomes shRNA-GFP or empty MigR1 by centrifugation (3,500 RPM, 24°C, 60 min) in sterile non-tissue culture plates treated with 20 µg/ml of plate-bound RetroNectin (Takara Bio Inc.). The next day, the cells were subjected to a second inoculation. After 4 d, the cells were FACS sorted on GFP^{high} DAPI^{low} population and either analyzed by flow cytometry, used as effectors in a cytotoxicity assay, or used in adoptive transferred experiments.

In vitro expansion of Trp1 cells and NY-ESO-1 CD4⁺ T cell lines.

NY-ESO-1 CD4⁺ T cell lines developed from three patients diagnosed with Stage IV melanoma were provided by S. Kitano. Approximately 1 × 10⁵ cells were expanded with 1 µg/ml of plate-bound anti-CD3 with or without anti-CD28 at 1 µg/ml (BD) in X-vivo 15 Media (BioWhittaker) supplemented with 10% heat inactivated human serum (Gemini Bio-products) and 30 U/ml IL-2 (Roche). Some wells were treated with 10 ng/ml of recombinant human OX40L-Fc (PeproTech). After 10 or 14 d, the expanded cells were subjected to in vitro cytotoxicity assays.

Trp1 cells were purified as described and 1 × 10⁵ cells were incubated with 3 × 10⁵ irradiated T cell-depleted splenocytes pulsed with 2.5 µg/ml of Trp1 peptide in HTM media. After 48 h, 10 µg/ml OX86 or IgG was added to the cultures. After 4 d, the cells were subjected to in vitro cytotoxicity assays.

Measurement of cytokines produced by Trp1 cells from treated mice *ex vivo*.

Mice were treated with the combination therapy as described previously. Single cell suspensions from tumors were incubated on ice with CD45.1 PE antibody (BD) for 15 min. Trp1 cells (CD45.1⁺) were further purified by with anti-PE MicroBeads (Miltenyi Biotec) according to the manufacturer's instructions. Purified Trp1 cells (5×10^4) were incubated with 1.5×10^5 irradiated T cell depleted splenocytes with 2.5 $\mu\text{g}/\text{ml}$ of Trp1 peptide in 200 μl HTM media. After 4 d, supernatants were assayed for Th1, Th2, and Th17 cytokines using the mouse Th1/Th2 10plex FlowCytomix Multiplex (eBioscience) according to the manufacturer's instructions.

Collagen I–fibrin gel *in vitro* cytotoxicity assay. Using a clonogenic assay to assess melanoma cell killing, Budhu et al. (2010) showed that collagen–fibrin gels were $\sim 5,000\times$ more sensitive in detecting cytotoxicity than conventional CTL killing assays. Therefore, we used collagen–fibrin gels along with the clonogenic assay to examine killing of melanoma cells by Trp1 cells and human NY-ESO-1 CD4⁺ T cell. Collagen–fibrin gels were formed, incubated, and lysed, and their contents of melanoma cells assayed exactly as previously described (Budhu et al., 2010). Target melanoma cells (with or without CD4⁺ T cells) were co-incubated in PBS containing 1 mg/ml human fibrinogen, 1 mg/ml rat tail collagen I, 10% FBS, and 0.1 U human thrombin. The gels were formed by incubating this mixture at 37°C for 20 min and then were overlaid with HTM media. 24 h later, the gels were lysed by sequential collagenase (2.5 mg/ml) and trypsin (2.5 mg/ml; Sigma–Aldrich) digestion. The lysed gels were then diluted and the recovered melanoma cells were plated in 6-well plates for colony formation. After 7–21 d in culture, the plates were fixed with formaldehyde, stained with 2% methylene blue, washed, dried, and the colonies were counted manually. A 10:1 effector to target ratio was used in all experiments. For the preparation of targets, B16 cells were incubated overnight with 10 ng/ml of recombinant IFN- γ (PeproTech) and single cell suspension were prepared using Cellstriper (Cellgro) before the assay. Human melanoma cell lines derived from three patients were incubated overnight with recombinant 10 ng/ml IFN- γ and single cell suspension was prepared with Cellstriper. To increase sensitivity the melanoma cells were pulsed with 10 $\mu\text{g}/\text{ml}$ of NY-ESO-1 peptides for 40 min at 37°C. The percentage of target cells killed was calculated using the equation: $1 - [\text{melanoma} + \text{T cells}]/[\text{melanoma alone}]$.

RT-PCR. Total RNA was extracted from CD4⁺ T cell lines with the RNeasy 96 kit (QIAGEN) and cDNA synthesized using High Capacity cDNA Reverse Transcription kit (Applied Biosystems) according to manufacturer's instructions. All primers and probes were from TaqMan Gene Expression Assays (Applied Biosystems). Real-time PCR reactions were prepared with 3 μl cDNA according to the manufacturer's instructions. All amplifications were done using the ABI 7500 Real Time PCR system (Applied Biosystems). Each gene was amplified in triplicate and cDNA concentration differences were normalized to GAPDH. Relative gene expression of the target genes were shown by $2^{-\Delta\text{Ct}}$ ($\Delta\text{Ct} = \text{Ct}(\text{target gene}) - \text{Ct}(\text{GAPDH})$) using mean Ct (threshold cycle) of triplicates.

Statistical analysis. Statistical differences between experimental groups were determined by the two-tailed Student's *t* test and Log-rank test using Prism software (GraphPad Software).

The authors wish to thank S. Terzulli for assistance in the creation of this manuscript and S.L. Reiner, G.A. Rizzuto, J.C. Sun, and A.M. Beaulieu for their helpful critical comments. We would like to thank A. Burey, X. Yang, and the members of the immunomonitoring facility at MSKCC for technical support. We also would like to thank the members of the Wolchok/Houghton Laboratory at MSKCC.

This work was supported by grants from the National Cancer Institute (R01 CA56821, P01 CA33049, and P01 CA59350), Swim Across America, the Lita Annenberg Hazen Foundation, the T.J. Martell Foundation, the Mr. William H. Goodwin and Mrs. Alice Goodwin and the Commonwealth Cancer Foundation for Research, and the Experimental Therapeutics Center of MSKCC.

The authors have no conflicting interests.

Submitted: 8 March 2012

Accepted: 27 August 2012

REFERENCES

- Al-Shamkhani, A., M.L. Birkeland, M. Puklavec, M.H. Brown, W. James, and A.N. Barclay. 1996. OX40 is differentially expressed on activated rat and mouse T cells and is the sole receptor for the OX40 ligand. *Eur. J. Immunol.* 26:1695–1699. <http://dx.doi.org/10.1002/eji.1830260805>
- Apetoh, L., F. Ghiringhelli, A. Tesniere, M. Obeid, C. Ortiz, A. Criollo, G. Mignot, M.C. Maiuri, E. Ullrich, P. Saulnier, et al. 2007. Toll-like receptor 4-dependent contribution of the immune system to anticancer chemotherapy and radiotherapy. *Nat. Med.* 13:1050–1059. <http://dx.doi.org/10.1038/nm1622>
- Awwad, M., and R.J. North. 1988. Cyclophosphamide (Cy)-facilitated adoptive immunotherapy of a Cy-resistant tumour. Evidence that Cy permits the expression of adoptive T-cell mediated immunity by removing suppressor T cells rather than by reducing tumour burden. *Immunology.* 65:87–92.
- Banerjee, A., S.M. Gordon, A.M. Intlekofer, M.A. Paley, E.C. Mooney, T. Lindsten, E.J. Wherry, and S.L. Reiner. 2010. Cutting edge: The transcription factor eomesodermin enables CD8⁺ T cells to compete for the memory cell niche. *J. Immunol.* 185:4988–4992. <http://dx.doi.org/10.4049/jimmunol.1002042>
- Belz, G.T., and A. Kallies. 2010. Effector and memory CD8⁺ T cell differentiation: toward a molecular understanding of fate determination. *Curr. Opin. Immunol.* 22:279–285. <http://dx.doi.org/10.1016/j.coi.2010.03.008>
- Bracci, L., F. Moschella, P. Sestili, V. La Sorsa, M. Valentini, I. Canini, S. Baccarini, S. Maccari, C. Ramoni, F. Belardelli, and E. Proietti. 2007. Cyclophosphamide enhances the antitumor efficacy of adoptively transferred immune cells through the induction of cytokine expression, B-cell and T-cell homeostatic proliferation, and specific tumor infiltration. *Clin. Cancer Res.* 13:644–653. <http://dx.doi.org/10.1158/1078-0432.CCR-06-1209>
- Brahmer, J.R., C.G. Drake, I. Wollner, J.D. Powderly, J. Picus, W.H. Sharfman, E. Stankevich, A. Pons, T.M. Salay, T.L. McMiller, et al. 2010. Phase I study of single-agent anti-programmed death-1 (MDX-1106) in refractory solid tumors: safety, clinical activity, pharmacodynamics, and immunologic correlates. *J. Clin. Oncol.* 28:3167–3175. <http://dx.doi.org/10.1200/JCO.2009.26.7609>
- Brode, S., and A. Cooke. 2008. Immune-potentiating effects of the chemotherapeutic drug cyclophosphamide. *Crit. Rev. Immunol.* 28:109–126. <http://dx.doi.org/10.1615/CritRevImmunol.v28.i2.20>
- Brown, D.M. 2010. Cytolytic CD4 cells: Direct mediators in infectious disease and malignancy. *Cell. Immunol.* 262:89–95. <http://dx.doi.org/10.1016/j.cellimm.2010.02.008>
- Budhu, S., J.D. Loike, A. Pandolfi, S. Han, G. Catalano, A. Constantinescu, R. Clynes, and S.C. Silverstein. 2010. CD8⁺ T cell concentration determines their efficiency in killing cognate antigen-expressing syngeneic mammalian cells *in vitro* and in mouse tissues. *J. Exp. Med.* 207:223–235. <http://dx.doi.org/10.1084/jem.20091279>
- Colombo, M.P., and S. Piconese. 2007. Regulatory-T-cell inhibition versus depletion: the right choice in cancer immunotherapy. *Nat. Rev. Cancer.* 7:880–887. <http://dx.doi.org/10.1038/nrc2250>
- Croft, M. 2010. Control of immunity by the TNFR-related molecule OX40 (CD134). *Annu. Rev. Immunol.* 28:57–78. <http://dx.doi.org/10.1146/annurev-immunol-030409-101243>
- Crotty, S., R.J. Johnston, and S.P. Schoenberger. 2010. Effectors and memories: Bcl-6 and Blimp-1 in T and B lymphocyte differentiation. *Nat. Immunol.* 11:114–120. <http://dx.doi.org/10.1038/ni.1837>
- Curiel, T.J. 2007. T regs and rethinking cancer immunotherapy. *J. Clin. Invest.* 117:1167–1174. <http://dx.doi.org/10.1172/JCI31202>
- Dudley, M.E., J.C. Yang, R. Sherry, M.S. Hughes, R. Royal, U. Kammula, P.F. Robbins, J. Huang, D.E. Citrin, S.F. Leitman, et al. 2008. Adoptive cell therapy for patients with metastatic melanoma: evaluation of intensive myeloablative chemoradiation preparative regimens. *J. Clin. Oncol.* 26:5233–5239. <http://dx.doi.org/10.1200/JCO.2008.16.5449>
- Dunn, G.P., A.T. Bruce, H. Ikeda, L.J. Old, and R.D. Schreiber. 2002. Cancer immunoediting: from immunosurveillance to tumor escape. *Nat. Immunol.* 3:991–998. <http://dx.doi.org/10.1038/ni1102-991>
- Eppihimer, M.J., J. Gunn, G.J. Freeman, E.A. Greenfield, T. Chernova, J. Erickson, and J.P. Leonard. 2002. Expression and regulation of the

- PD-L1 immunoinhibitory molecule on microvascular endothelial cells. *Microcirculation*. 9:133–145.
- Graf, L.H. Jr., P. Kaplan, and S. Silagi. 1984. Efficient DNA-mediated transfer of selectable genes and unselected sequences into differentiated and undifferentiated mouse melanoma clones. *Somat. Cell Mol. Genet.* 10:139–151. <http://dx.doi.org/10.1007/BF01534903>
- Gramaglia, I., A. Jember, S.D. Pippig, A.D. Weinberg, N. Killeen, and M. Croft. 2000. The OX40 costimulatory receptor determines the development of CD4 memory by regulating primary clonal expansion. *J. Immunol.* 165:3043–3050.
- Grupp, S.A., and C.H. June. 2011. Adoptive cellular therapy. *Curr. Top. Microbiol. Immunol.* 344:149–172. http://dx.doi.org/10.1007/82_2010_94
- Hegazy, A.N., M. Peine, C. Helmstetter, I. Panse, A. Fröhlich, A. Bergthaler, L. Flatz, D.D. Pinschewer, A. Radbruch, and M. Löhning. 2010. Interferons direct Th2 cell reprogramming to generate a stable GATA-3(+)T-bet(+) cell subset with combined Th2 and Th1 cell functions. *Immunity*. 32:116–128. <http://dx.doi.org/10.1016/j.immuni.2009.12.004>
- Hirschhorn-Cymerman, D., G.A. Rizzuto, T. Merghoub, A.D. Cohen, F. Avogadri, A.M. Lesokhin, A.D. Weinberg, J.D. Wolchok, and A.N. Houghton. 2009. OX40 engagement and chemotherapy combination provides potent antitumor immunity with concomitant regulatory T cell apoptosis. *J. Exp. Med.* 206:1103–1116. <http://dx.doi.org/10.1084/jem.20082205>
- Hodi, F.S., S.J. O'Day, D.F. McDermott, R.W. Weber, J.A. Sosman, J.B. Haanen, R. Gonzalez, C. Robert, D. Schadendorf, J.C. Hassel, et al. 2010. Improved survival with ipilimumab in patients with metastatic melanoma. *N. Engl. J. Med.* 363:711–723. <http://dx.doi.org/10.1056/NEJMoa1003466>
- Houot, R., and R. Levy. 2009. T-cell modulation combined with intratumoral CpG cures lymphoma in a mouse model without the need for chemotherapy. *Blood*. 113:3546–3552. <http://dx.doi.org/10.1182/blood-2008-07-170274>
- Hunder, N.N., H. Wallen, J. Cao, D.W. Hendricks, J.Z. Reilly, R. Rodmyre, A. Jungbluth, S. Gnjatic, J.A. Thompson, and C. Yee. 2008. Treatment of metastatic melanoma with autologous CD4+ T cells against NY-ESO-1. *N. Engl. J. Med.* 358:2698–2703. <http://dx.doi.org/10.1056/NEJMoa0800251>
- Ichiyama, K., T. Sekiya, N. Inoue, T. Tamiya, I. Kashiwagi, A. Kimura, R. Morita, G. Muto, T. Shichita, R. Takahashi, and A. Yoshimura. 2011. Transcription factor Smad-independent T helper 17 cell induction by transforming-growth factor- β is mediated by suppression of eomesodermin. *Immunity*. 34:741–754. <http://dx.doi.org/10.1016/j.immuni.2011.02.021>
- Johnston, R.J., A.C. Poholek, D. DiToro, I. Yusuf, D. Eto, B. Barnett, A.L. Dent, J. Craft, and S. Crotty. 2009. Bcl6 and Blimp-1 are reciprocal and antagonistic regulators of T follicular helper cell differentiation. *Science*. 325:1006–1010. <http://dx.doi.org/10.1126/science.1175870>
- June, C.H. 2007. Principles of adoptive T cell cancer therapy. *J. Clin. Invest.* 117:1204–1212. <http://dx.doi.org/10.1172/JCI31446>
- Ko, K., S. Yamazaki, K. Nakamura, T. Nishioka, K. Hirota, T. Yamaguchi, J. Shimizu, T. Nomura, T. Chiba, and S. Sakaguchi. 2005. Treatment of advanced tumors with agonistic anti-GITR mAb and its effects on tumor-infiltrating Foxp3⁺CD25⁺CD4⁺ regulatory T cells. *J. Exp. Med.* 202:885–891. <http://dx.doi.org/10.1084/jem.20050940>
- Kress, S., J. König, J. Schweizer, H. Löhrike, R. Bauer-Hofmann, and M. Schwarz. 1992. p53 mutations are absent from carcinogen-induced mouse liver tumors but occur in cell lines established from these tumors. *Mol. Carcinog.* 6:148–158. <http://dx.doi.org/10.1002/mc.2940060210>
- Lee, J., M. Sadelain, and R. Brentjens. 2009. Retroviral transduction of murine primary T lymphocytes. *Methods Mol. Biol.* 506:83–96. http://dx.doi.org/10.1007/978-1-59745-409-4_7
- Moon, J.J., H.H. Chu, M. Pepper, S.J. McSorley, S.C. Jameson, R.M. Kedl, and M.K. Jenkins. 2007. Naive CD4(+) T cell frequency varies for different epitopes and predicts repertoire diversity and response magnitude. *Immunity*. 27:203–213. <http://dx.doi.org/10.1016/j.immuni.2007.07.007>
- Muranski, P., and N.P. Restifo. 2009. Adoptive immunotherapy of cancer using CD4(+) T cells. *Curr. Opin. Immunol.* 21:200–208. <http://dx.doi.org/10.1016/j.coi.2009.02.004>
- Muranski, P., A. Boni, P.A. Antony, L. Cassard, K.R. Irvine, A. Kaiser, C.M. Paulos, D.C. Palmer, C.E. Touloukian, K. Ptak, et al. 2008. Tumor-specific Th17-polarized cells eradicate large established melanoma. *Blood*. 112:362–373. <http://dx.doi.org/10.1182/blood-2007-11-120998>
- North, R.J. 1982. Cyclophosphamide-facilitated adoptive immunotherapy of an established tumor depends on elimination of tumor-induced suppressor T cells. *J. Exp. Med.* 155:1063–1074. <http://dx.doi.org/10.1084/jem.155.4.1063>
- Nowak, A.K., R.A. Lake, A.L. Marzo, B. Scott, W.R. Heath, E.J. Collins, J.A. Freilinger, and B.W. Robinson. 2003. Induction of tumor cell apoptosis in vivo increases tumor antigen cross-presentation, cross-priming rather than cross-tolerizing host tumor-specific CD8 T cells. *J. Immunol.* 170:4905–4913.
- O'Shea, J.J., and W.E. Paul. 2010. Mechanisms underlying lineage commitment and plasticity of helper CD4+ T cells. *Science*. 327:1098–1102. <http://dx.doi.org/10.1126/science.1178334>
- Overwijk, W.W., M.R. Theoret, S.E. Finkelstein, D.R. Surman, L.A. de Jong, F.A. Vyth-Dreese, T.A. DelleMijn, P.A. Antony, P.J. Spiess, D.C. Palmer, et al. 2003. Tumor regression and autoimmunity after reversal of a functionally tolerant state of self-reactive CD8+ T cells. *J. Exp. Med.* 198:569–580. <http://dx.doi.org/10.1084/jem.20030590>
- Pearce, E.L., A.C. Mullen, G.A. Martins, C.M. Krawczyk, A.S. Hutchins, V.P. Zediak, M. Banica, C.B. DiCioccio, D.A. Gross, C.A. Mao, et al. 2003. Control of effector CD8+ T cell function by the transcription factor Eomesodermin. *Science*. 302:1041–1043. <http://dx.doi.org/10.1126/science.1090148>
- Piconese, S., B. Valzasina, and M.P. Colombo. 2008. OX40 triggering blocks suppression by regulatory T cells and facilitates tumor rejection. *J. Exp. Med.* 205:825–839. <http://dx.doi.org/10.1084/jem.20071341>
- Quezada, S.A., K.S. Peggs, M.A. Curran, and J.P. Allison. 2006. CTLA4 blockade and GM-CSF combination immunotherapy alters the intratumor balance of effector and regulatory T cells. *J. Clin. Invest.* 116:1935–1945. <http://dx.doi.org/10.1172/JCI27745>
- Quezada, S.A., T.R. Simpson, K.S. Peggs, T. Merghoub, J. Vider, X. Fan, R. Blasberg, H. Yagita, P. Muranski, P.A. Antony, et al. 2010. Tumor-reactive CD4+ T cells develop cytotoxic activity and eradicate large established melanoma after transfer into lymphopenic hosts. *J. Exp. Med.* 207:637–650. <http://dx.doi.org/10.1084/jem.20091918>
- Qui, H.Z., A.T. Hagymasi, S. Bandyopadhyay, M.C. St Rose, R. Ramanarasimhaiah, A. Ménoiret, R.S. Mittler, S.M. Gordon, S.L. Reiner, A.T. Vella, and A.J. Adler. 2011. CD134 plus CD137 dual costimulation induces Eomesodermin in CD4 T cells to program cytotoxic Th1 differentiation. *J. Immunol.* 187:3555–3564. <http://dx.doi.org/10.4049/jimmunol.1101244>
- Redmond, W.L., C.E. Ruby, and A.D. Weinberg. 2009. The role of OX40-mediated co-stimulation in T-cell activation and survival. *Crit. Rev. Immunol.* 29:187–201. <http://dx.doi.org/10.1615/CritRevImmunol.v29.i3.10>
- Rizzuto, G.A., T. Merghoub, D. Hirschhorn-Cymerman, C. Liu, A.M. Lesokhin, D. Sahawneh, H. Zhong, K.S. Panageas, M.A. Perales, G. Altan-Bonnet, et al. 2009. Self-antigen-specific CD8+ T cell precursor frequency determines the quality of the antitumor immune response. *J. Exp. Med.* 206:849–866. <http://dx.doi.org/10.1084/jem.20081382>
- Robert, C., L. Thomas, I. Bondarenko, S. O'Day, J.W. M D, C. Garbe, C. Lebbe, J.F. Baurain, A. Testori, J.J. Grob, et al. 2011. Ipilimumab plus dacarbazine for previously untreated metastatic melanoma. *N. Engl. J. Med.* 364:2517–2526. <http://dx.doi.org/10.1056/NEJMoa1104621>
- Rogers, P.R., J. Song, I. Gramaglia, N. Killeen, and M. Croft. 2001. OX40 promotes Bcl-xL and Bcl-2 expression and is essential for long-term survival of CD4 T cells. *Immunity*. 15:445–455. [http://dx.doi.org/10.1016/S1074-7613\(01\)00191-1](http://dx.doi.org/10.1016/S1074-7613(01)00191-1)
- Rolink, A., F. Melchers, and J. Andersson. 1996. The SCID but not the RAG-2 gene product is required for S mu-S epsilon heavy chain class switching. *Immunity*. 5:319–330. [http://dx.doi.org/10.1016/S1074-7613\(00\)80258-7](http://dx.doi.org/10.1016/S1074-7613(00)80258-7)
- Rosenberg, S.A., N.P. Restifo, J.C. Yang, R.A. Morgan, and M.E. Dudley. 2008. Adoptive cell transfer: a clinical path to effective cancer immunotherapy. *Nat. Rev. Cancer*. 8:299–308. <http://dx.doi.org/10.1038/nrc2355>
- Ruby, C.E., M.A. Yates, D. Hirschhorn-Cymerman, P. Chlebeck, J.D. Wolchok, A.N. Houghton, H. Offner, and A.D. Weinberg. 2009. Cutting edge: OX40 agonists can drive regulatory T cell expansion if the cytokine milieu is right. *J. Immunol.* 183:4853–4857. <http://dx.doi.org/10.4049/jimmunol.0901112>

- Spiotto, M.T., D.A. Rowley, and H. Schreiber. 2004. Bystander elimination of antigen loss variants in established tumors. *Nat. Med.* 10:294–298. <http://dx.doi.org/10.1038/nm999>
- Stromnes, I.M., J.N. Blattman, X. Tan, S. Jeevanjee, H. Gu, and P.D. Greenberg. 2010. Abrogating Cbl-b in effector CD8(+) T cells improves the efficacy of adoptive therapy of leukemia in mice. *J. Clin. Invest.* 120:3722–3734. <http://dx.doi.org/10.1172/JCI41991>
- Trapani, J.A., and M.J. Smyth. 2002. Functional significance of the perforin/granzyme cell death pathway. *Nat. Rev. Immunol.* 2:735–747. <http://dx.doi.org/10.1038/nri911>
- van der Most, R.G., A.J. Currie, A.L. Cleaver, J. Salmons, A.K. Nowak, S. Mahendran, I. Larma, A. Prosser, B.W. Robinson, M.J. Smyth, et al. 2009. Cyclophosphamide chemotherapy sensitizes tumor cells to TRAIL-dependent CD8 T cell-mediated immune attack resulting in suppression of tumor growth. *PLoS ONE.* 4:e6982. <http://dx.doi.org/10.1371/journal.pone.0006982>
- Vu, M.D., X. Xiao, W. Gao, N. Degauque, M. Chen, A. Kroemer, N. Killeen, N. Ishii, and X.C. Li. 2007. OX40 costimulation turns off Foxp3+ T regs. *Blood.* 110:2501–2510. <http://dx.doi.org/10.1182/blood-2007-01-070748>
- Weinberg, A.D., M.M. Rivera, R. Prell, A. Morris, T. Ramstad, J.T. Vetto, W.J. Urba, G. Alvord, C. Bunce, and J. Shields. 2000. Engagement of the OX-40 receptor in vivo enhances antitumor immunity. *J. Immunol.* 164:2160–2169.
- Weinberg, A.D., N.P. Morris, M. Kovacsovics-Bankowski, W.J. Urba, and B.D. Curti. 2011. Science gone translational: the OX40 agonist story. *Immunol. Rev.* 244:218–231. <http://dx.doi.org/10.1111/j.1600-065X.2011.01069.x>
- Wherry, E.J. 2011. T cell exhaustion. *Nat. Immunol.* 12:492–499. <http://dx.doi.org/10.1038/ni.2035>
- Wolchok, J.D., B. Neyns, G. Linette, S. Negrier, J. Lutzky, L. Thomas, W. Waterfield, D. Schadendorf, M. Smylie, T. Guthrie Jr., et al. 2010. Ipilimumab monotherapy in patients with pretreated advanced melanoma: a randomised, double-blind, multicentre, phase 2, dose-ranging study. *Lancet Oncol.* 11:155–164. [http://dx.doi.org/10.1016/S1470-2045\(09\)70334-1](http://dx.doi.org/10.1016/S1470-2045(09)70334-1)
- Wrzesinski, C., and N.P. Restifo. 2005. Less is more: lymphodepletion followed by hematopoietic stem cell transplant augments adoptive T-cell-based anti-tumor immunotherapy. *Curr. Opin. Immunol.* 17:195–201. <http://dx.doi.org/10.1016/j.coi.2005.02.002>
- Xie, Y., A. Akpınarlı, C. Maris, E.L. Hipkiss, M. Lane, E.K. Kwon, P. Muranski, N.P. Restifo, and P.A. Antony. 2010. Naive tumor-specific CD4+ T cells differentiated in vivo eradicate established melanoma. *J. Exp. Med.* 207:651–667. <http://dx.doi.org/10.1084/jem.20091921>
- Zhou, L., M.M. Chong, and D.R. Littman. 2009. Plasticity of CD4+ T cell lineage differentiation. *Immunity.* 30:646–655. <http://dx.doi.org/10.1016/j.immuni.2009.05.001>
- Zhou, X., S. Yu, D.M. Zhao, J.T. Harty, V.P. Badovinac, and H.H. Xue. 2010. Differentiation and persistence of memory CD8(+) T cells depend on T cell factor 1. *Immunity.* 33:229–240. <http://dx.doi.org/10.1016/j.immuni.2010.08.002>
- Zhu, J., H. Yamane, and W.E. Paul. 2010. Differentiation of effector CD4 T cell populations (*). *Annu. Rev. Immunol.* 28:445–489. <http://dx.doi.org/10.1146/annurev-immunol-030409-101212>